The Astrophysical Journal, 687:1168–1179, 2008 November 10

CO FUNDAMENTAL EMISSION FROM V836 TAURI[1]

Joan R. Najita and Nathan Crockett
National Optical Astronomy Observatory, 950 North Cherry Avenue, Tucson, AZ 85719

and

John S. Carr
Naval Research Laboratory, Code 7213, Washington, DC 20375
Received 2008 May 20; accepted 2008 July 14

ABSTRACT

We present high-resolution 4.7 μm CO fundamental spectroscopy of V836 Tau, a young star with properties that are between those of classical and weak T Tauri stars and which may be dissipating its circumstellar disk. We find that the CO line profiles of V836 Tau are unusual in that they are markedly double-peaked, even after correcting for stellar photospheric absorption in the spectrum. This suggests that the CO emission arises from a restricted range of disk radii ($<$0.5 AU), in contrast to the situation for most classical T Tauri stars, where the CO emission extends out to much larger radii ($\sim$1–2 AU). We discuss whether the outer radius of the emission in V836 Tau results from the physical truncation of the disk or an excitation effect. We also explore how either of these hypotheses may bear on our understanding of disk dissipation in this system.

Subject headings: circumstellar matter — planetary systems: formation — planetary systems: protoplanetary disks — stars: individual (V836 Tauri) — stars: pre–main-sequence

Online material: color figures

1. INTRODUCTION

V836 Tau is an interesting young star with properties that are between those of classical and weak T Tauri stars. Its optical spectrum displays relatively weak, variable Hα emission, with measured equivalent widths in the range 1–25 Å (White & Hillenbrand 2004; Beristain et al. 2001; Kenyon et al. 1998; Wolk & Walter 1996; Mundt et al. 1983). Similarly, V836 Tau also shows little veiling and has one of the smallest measured stellar accretion rates among T Tauri stars (Hartigan et al. 1995). Nevertheless, the detection of Hα emission with an inverse P Cygni profile (Wolk & Walter 1996) demonstrates the continued, possibly intermittent, accretion of material onto the star. Millimeter wavelength CO emission has also been detected from V836 Tau (Duvert et al. 2000) despite the relatively low disk mass $\sim$0.01 $M_\odot$ inferred from the submillimeter dust continuum properties (e.g., Andrews & Williams 2005).

At infrared wavelengths, V836 shows little or no excess in the K and L bands, but a much stronger excess indicative of an optically thick disk is apparent beyond 10 μm (Strom et al. 1989; Skrutskie et al. 1990; Padgett et al. 2006). Interpreting the unusual spectral energy distribution (SED) and low stellar accretion rate of V836 Tau as indications that the system is on the verge of dissipating its disk, Strom et al. (1989) consequently referred to V836 Tau as a "transitional T Tauri star," a term reflecting the view that classical T Tauri stars evolve into weak T Tauri stars, with the dissipation of the disk playing a central role in that evolutionary process. More generally, transition objects, systems that can be modeled as an optically thick disk that has an optically thin region (a hole or a gap) at smaller radii, have been suggested to be in the process of dissipating their disks from the inside-out (Strom et al. 1989; Skrutskie et al. 1990), possibly as a result of the formation of planetesimals (Strom et al. 1989), a giant planetary companion (e.g., Skrutskie et al. 1990), disk photoevaporation (Clarke et al. 2001; Alexander et al. 2006), or potentially other processes.

We report here on the properties of the 4.7 μm CO fundamental ($\Delta v = 1$) emission from V836 Tau to see whether it can provide any insights into the extent and nature of disk dissipation in the system. CO fundamental emission has been previously characterized as a probe of circumstellar disk gas (Najita et al. 2003, 2007a; Blake & Boogert 2004; Brittain et al. 2007). In the case of disks surrounding low-mass stars, CO fundamental emission is estimated to arise from within 1–2 AU of the star (Najita et al. 2003). As a result, the emission is well suited to probing the radial distribution of gas in the terrestrial planet region of the disk. Recent thermal-chemical models of the inner regions of disks surrounding low-mass stars suggest that the CO emission arises from the warm surface region of the disk that is heated by stellar (X-ray) irradiation and possibly mechanical heating processes (e.g., Glassgold et al. 2004). The CO fundamental emission from V836 Tau was discussed briefly in an earlier study (Najita et al. 2003). Here we report a new, higher signal-to-noise observation of the CO emission, which we use to characterize the radial distribution of the gas in inner $\sim$1–2 AU of the disk surrounding V836 Tau.

2. OBSERVATIONS

We obtained a high-resolution ($R = 25{,}000$) spectrum of V836 Tau on the night of 2003 January 11 at the W. M. Keck Observatory using NIRSPEC (McLean et al. 1998) in echelle mode with a 0.43″ slit. Our spectral setup included two echelle orders covering the spectral ranges 4.586–4.662 μm (in order 16) and

[1] The data presented herein were obtained at the W. M. Keck Observatory from telescope time allocated to NASA through the agency's scientific partnership with the California Institute of Technology and the University of California. The Observatory was made possible by the generous financial support of the W. M. Keck Foundation.

Report Documentation Page

Form Approved
OMB No. 0704-0188

1. REPORT DATE	2. REPORT TYPE	3. DATES COVERED
NOV 2008		**00-00-2008 to 00-00-2008**

4. TITLE AND SUBTITLE	5a. CONTRACT NUMBER
CO Fundamental Emission from V836 Tauri	5b. GRANT NUMBER
	5c. PROGRAM ELEMENT NUMBER
6. AUTHOR(S)	5d. PROJECT NUMBER
	5e. TASK NUMBER
	5f. WORK UNIT NUMBER
7. PERFORMING ORGANIZATION NAME(S) AND ADDRESS(ES) **Naval Research Laboratory,Code 7213,Washington,DC,20375**	8. PERFORMING ORGANIZATION REPORT NUMBER
9. SPONSORING/MONITORING AGENCY NAME(S) AND ADDRESS(ES)	10. SPONSOR/MONITOR'S ACRONYM(S)
	11. SPONSOR/MONITOR'S REPORT NUMBER(S)

12. DISTRIBUTION/AVAILABILITY STATEMENT
Approved for public release; distribution unlimited

13. SUPPLEMENTARY NOTES

14. ABSTRACT
see report

15. SUBJECT TERMS

16. SECURITY CLASSIFICATION OF:			17. LIMITATION OF ABSTRACT	18. NUMBER OF PAGES	19a. NAME OF RESPONSIBLE PERSON
a. REPORT **unclassified**	b. ABSTRACT **unclassified**	c. THIS PAGE **unclassified**	**Same as Report (SAR)**	**12**	

4.890–4.972 μm (in order 15). These wavelength regions include low-J CO $v = 1-0$ R-branch transitions in order 16 and high-J CO $v = 1-0$ P-branch transitions in order 15. Observations at 4.7 μm are dominated by strong thermal background continuum and telluric emission lines. In order to remove these features, the telescope was nodded in an ABBA pattern at 2 minute intervals between two positions in the slit separated by 12″. During our observations, the seeing varied between ~0.6″ and ~1.1″, mainly as a result of high wind. As a result, the total effective integration time on the source was 40 minutes. In addition, fixed pattern noise on the left two quadrants of the detector increased the noise in these quadrants by a factor of ~1.5 relative to the noise on the right side of the array. This reduced the signal-to-noise ratio in the short-wavelength half of each order.

All data reduction procedures were carried out using IRAF. Subsequent images were subtracted from each other, removing the background and telluric emission lines to first order. A flat-field correction was applied to each differenced image. To minimize the impact of imperfectly canceled telluric emission lines on the extracted spectrum, we rectified the images so that the image of the slit ran vertically along pixel columns. The required geometric transformation was obtained from the original pattern of telluric emission lines using the IRAF tasks `fitcoords` and `transform`. Individual differenced images were average combined and one-dimensional spectra were extracted for each nod position and order. Because the spectra had been rectified, large background apertures (located on both sides of the source aperture) could be used in extracting the spectrum, producing a higher signal-to-noise spectrum.

Telluric absorption features were removed by dividing the program spectrum by that of a telluric standard (the hot star HR 1605; spectral type A8), which was obtained and reduced in the same way as the V836 Tau spectrum. The spectrum of HR 1605 was mostly featureless except for absorption in the 7–5 Pfβ line. Consequently, the divided spectrum has artificially enhanced hydrogen emission in this region. To correct for the difference in air mass between the object and the standard spectra, we used the IRAF task `telluric` to perform the division.

Telluric absorption lines were used for the wavelength calibration. An approximate flux calibration was obtained by acquiring additional spectra of both V836 Tau and HR 1605 with the 0.72″ NIRSPEC slit. Given the poor seeing, slit losses are likely to have been significant. The short integrations used for the V836 Tau observations result in a formal 1 σ error of 25% in the flux calibration of each order. The possibility of slit losses contributes additional uncertainty in the flux.

Nevertheless, the resulting continuum fluxes for each order agree to ~15% with the 4.5 μm *Spitzer* IRAC flux reported for V836 Tau (Padgett et al. 2006; [$F_{4.5} = 0.127$ Jy]). For comparison, our calibrated continuum flux of 0.128 Jy, the average of the continuum level in orders 15 and 16, is ~80% brighter than the value of ~0.07 Jy that we reported previously for V836 Tau in the same wavelength region based on NIRSPEC data taken in 2001 (Najita et al. 2003). It is also 30% fainter than the 0.18 Jy continuum flux at 4.78 μm that is implied by extrapolating the *Spitzer* IRS spectrum of V836 Tau (Furlan et al. 2006) to that wavelength. Because of the relatively large uncertainty in the flux calibration for each order, we are unable to determine if there is a shallow continuum slope between the two orders. We therefore adopted the continuum flux slope measured by Furlan et al. and scaled the flux so that the average of the continuum fluxes at the wavelength centers of orders 15 and 16 agrees with our measured average value.

We also acquired on 2004 November 23 similar NIRSPEC spectra of the K5 V star 61 Cyg A. These spectra were used in calibrating synthetic models of the stellar photospheric contribution to the V836 Tau spectrum (see § 3.1). The data were reduced and wavelength calibrated with the same procedure used for the V836 Tau data.

3. RESULTS

The resulting CO fundamental spectrum is of significantly higher signal-to-noise than our previously reported spectrum of V836 Tau (Najita et al. 2003). In the earlier spectrum, CO emission was clearly detected, but the shape of the line profile was unclear and the properties of the emission were unusual. The line widths of the low-J R lines were found to be significantly narrower than the widths of the high-J P lines (41 km s^{-1} compared to 58 km s^{-1}). In addition, the emission at 4.6 μm appeared to peak at a radial velocity redward of the stellar velocity. A comparison with the new spectrum shows that this was because the blue component of the low-J profiles was not recovered in the earlier data, a result of our limited ability to correct for telluric absorption given the lower signal-to-noise of the earlier data. The new, higher signal-to-noise data show $v = 1-0$ emission that is double-peaked in both the 4.6 and 4.9 μm regions (Figs. 1 and 2, respectively, *top panels*) and centered at the radial velocity of the star. The emission equivalent width is comparable to that in the earlier spectrum.

The double-peaked line profiles of the CO $v = 1-0$ emission from V836 Tau are unusual in that the majority of classical T Tauri stars that have been studied to date show CO $v = 1-0$ line profiles that are centrally peaked (Najita et al. 2003). For emission arising in a disk, double-peaked profiles indicate that the emission arises from a limited range of disk radii. For example, this is the interpretation given to the double-peaked 2.3 μm CO overtone ($\Delta v = 2$) emission lines that are observed from actively accreting young stars (e.g., WL 16, DG Tau; Carr et al. 1993; Najita et al. 1996, 2000).

3.1. *Stellar Photosphere Component*

Because the observed spectrum is a composite of the emission from the star and disk, some fraction of the central dip in the CO line profile may result from absorption in the stellar photospheric component. We estimated the stellar contribution to the spectrum using the recent version of the stellar spectral synthesis program MOOG (Sneden 1973). As inputs, we used the NextGen model atmospheres (Hauschildt et al. 1999) and the CO line list of Goorvitch (1994). The ability to fit the CO spectrum in this wavelength region was verified on a spectrum of the K5 dwarf 61 Cyg A, which was obtained with the same instrumental setup as the spectrum of V836 Tau. For our adopted stellar parameters for 61 Cyg A ($T = 4400$ K, $\log g = 4.5$) and near-solar metallicities, we obtain an excellent fit to the spectrum. In contrast, with the atmospheric models of Kurucz (1993), it is not possible to match the relative strengths of the weak and strong CO lines.

We selected an atmosphere model that is appropriate for the stellar photospheric temperature ($T_{\rm eff} = 4000$ K) and gravity ($\log g = 4.0$), which are implied by the stellar effective temperature and luminosity of V836 Tau measured by White & Hillenbrand (2004). We adopted a solar metallicity, as appropriate for the Taurus star-forming region (Padgett 1996; Santos et al. 2008).

A comparison of the synthetic stellar spectrum and the observed spectrum of V836 Tau shows that much of the structure in

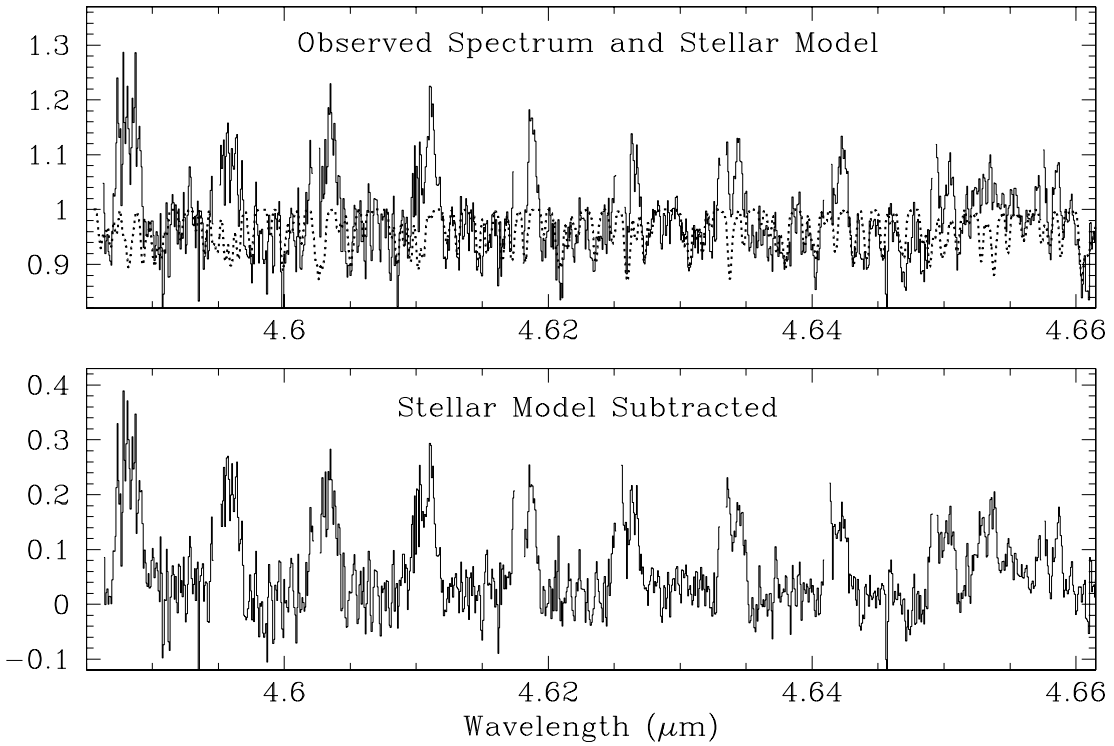

FIG. 1.—Observed spectrum of V836 Tau in the 4.6 μm region, normalized to the continuum level (*top panel, histogram*). The adopted synthetic stellar photospheric spectrum with a veiling continuum level that is constant with wavelength is also shown (*dotted line*). The CO emission spectrum from the disk (in continuum flux units; *bottom panel*) is obtained by subtracting the veiled stellar photosphere from the observed spectrum. In both panels, regions of the spectrum that have poor telluric correction are not plotted. Note that hydrogen 7–5 Pfβ absorption was present in the telluric standard used to calibrate the data. Since we did not attempt to correct for the absorption, the hydrogen line emission at 4.654 μm is artificially enhanced. [*See the electronic edition of the Journal for a color version of this figure.*]

the continuum is due to absorption features in the stellar photosphere (Figs. 1 and 2, *top panels*). Stellar photospheric features are expected to be detectable in high signal-to-noise spectra given the weak near-infrared excess of V836 Tau. The heliocentric radial velocity of 18.5 km s^{-1} (which corresponds to a topocentric velocity of $v_{\rm obs} = 35.5$ km s^{-1}) and the stellar rotational velocity of $v \sin i \simeq 12.1$ km s^{-1} measured by White & Hillenbrand (2004) are in agreement with the stellar photospheric features identified in the observed spectrum. These parameters, combined with a continuum veiling of $r_{4.7} = 2$ (where $r_{4.7}$ is the ratio of the

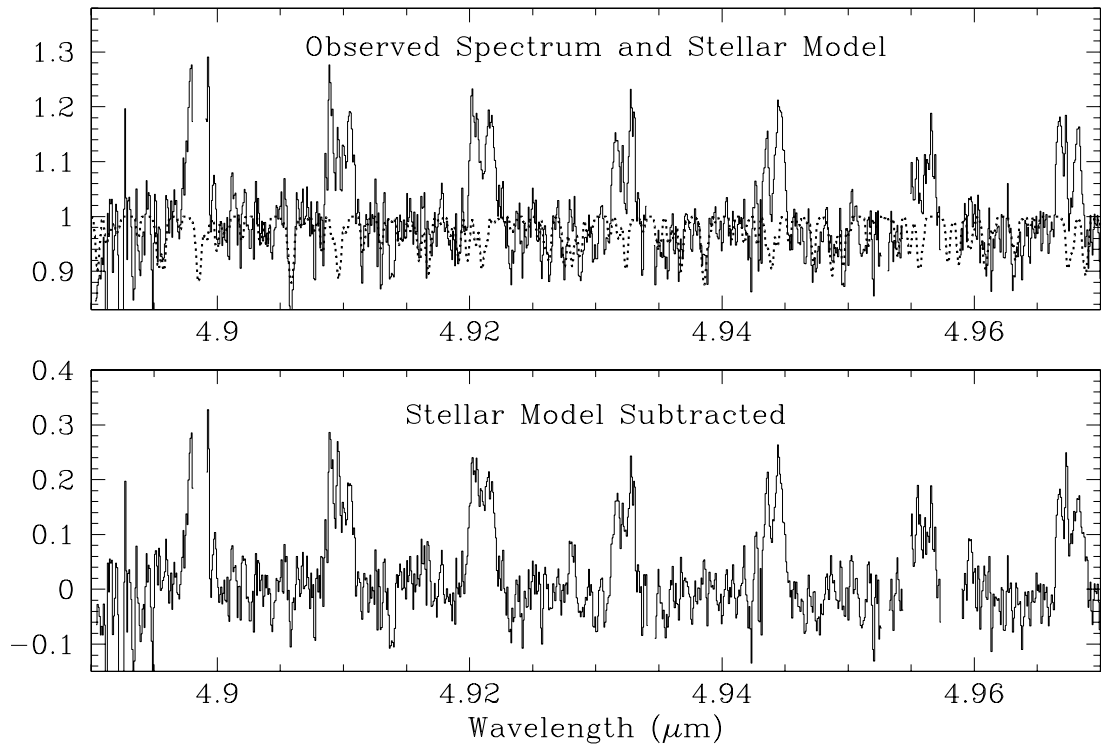

FIG. 2.—Same as in Fig. 1, but for the 4.9 μm region. [*See the electronic edition of the Journal for a color version of this figure.*]

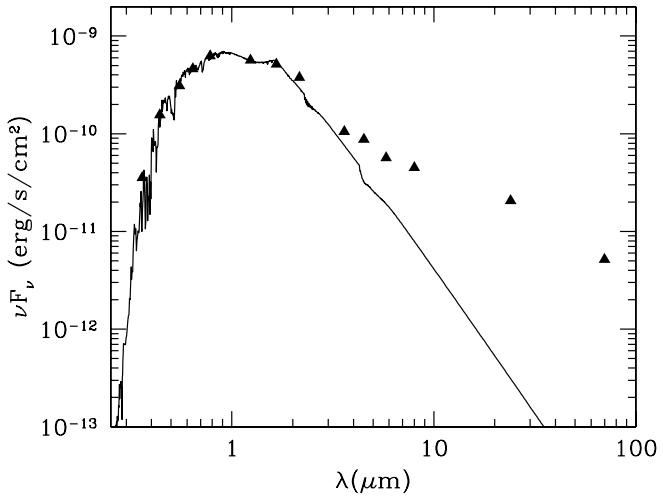

FIG. 3.—SED of V836 Tau based on photometry in the literature and dereddened assuming $A_V = 1.1$ (*triangles*; see text for details). A Basel model atmosphere (ver. 2.2, corrected) for $T_{\rm eff} = 4060$ K and $\log g = 4.0$ (*solid line*) is shown for comparison.

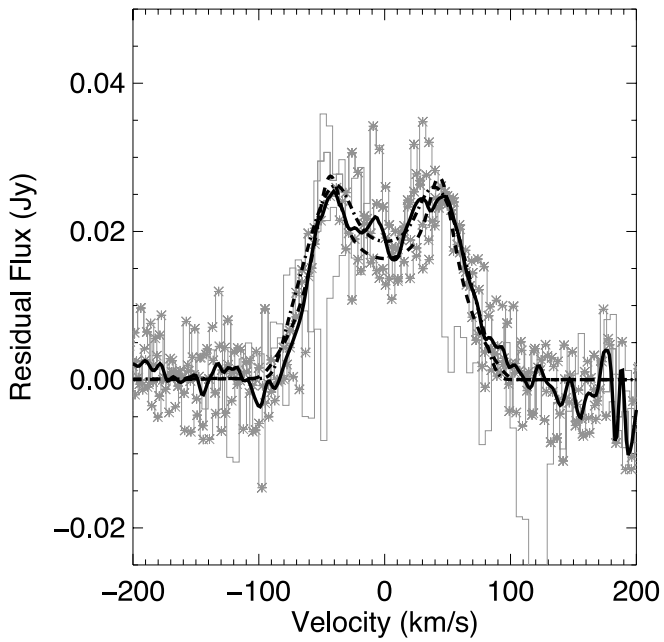

FIG. 4.—Average CO emission profile from V836 Tau in the 4.9 μm region (*heavy solid black line*) compared with a synthetic disk emission profile for the $v = 1{-}0$ *P*26 line in a model that has an outer radius to the emission (*dashed line*; see Fig. 6 and text for details). The synthetic *P*26 line profile for a model with a steep temperature gradient (*dash-dotted line*) is also shown (see text for details). The velocities shown are relative to the V836 Tau stellar velocity. The individual lines that contribute to the average (1–0 *P*25–*P*28 and *P*30) are shown as gray histograms. Points included in the average are indicated by asterisks. The average profile is symmetric, double-peaked, and centered at the stellar velocity. [*See the electronic edition of the Journal for a color version of this figure*.]

excess flux to the stellar photospheric flux at 4.7 μm), provides a reasonably good fit to the observed spectrum. The depth of the CO absorption in the veiled stellar photospheric spectrum shows that some of the central absorption in the observed CO emission profile arises from CO absorption in the stellar photosphere.

The measured veiling has two sources of uncertainty. The low signal-to-noise of the spectrum introduces uncertainty in the location of the continuum, contributing an uncertainty of ± 0.3 to the veiling measurement. The uncertainty in the stellar effective temperature (± 200 K) and $\log g$ (± 0.3) of V836 Tau (see § 3.3) contributes an additional uncertainty of ± 0.16 to the veiling.

Figure 3 shows the dereddened SED of V836 Tau. We constructed the SED from the *UBVRI* photometry of Kenyon & Hartmann (1995), the *JHK* fluxes from 2MASS, and the *Spitzer* IRAC and MIPS photometry reported by Padgett et al. (2006). The fluxes were dereddened using the reddening law of Mathis (1990), assuming $A_V = 1.1$ as in Furlan et al. (2006). A Basel stellar atmosphere (ver. 2.2, corrected; Lejeune 2002) with $T_{\rm eff} = 4060$ K and $\log g = 4.0$ provides a good fit to the dereddened optical colors of the star. The stellar contribution as shown is roughly consistent with the minimal veiling at *R* and *I* measured by White & Hillenbrand (2004). Overall, the SED is approximately photospheric below 3.5 μm, with a significant infrared excess beyond that wavelength.

Our measured veiling of $r_{4.7} = 2$ is consistent with values that are implied by the stellar photospheric contribution to the SED shown in Figure 3 and photometric measurements of V836 Tau in the literature. For consistency with the stellar photospheric contribution to the SED, our veiling requires a continuum flux of $\sim$0.16 Jy at the time our spectrum was obtained, which is within the level of uncertainty in our flux calibration.

3.2. CO *Emission-Line Profile*

To obtain the disk contribution to the CO fundamental spectrum, we subtracted the veiled stellar photosphere from the observed spectrum (Figs. 1 and 2, *bottom panels*). The difference spectrum shows that even after accounting for stellar photospheric absorption, the residual CO emission spectrum has a double-peaked line profile. We can better define the line profile by averaging multiple CO emission lines to improve the signal-to-noise of the line profile. In constructing an average line profile, regions of poor telluric correction (below a cutoff value of 90%–95% transmission) were excluded from the average. The regions to exclude were determined from the observations of the telluric standard.

The average profiles of the low-*J R* and high-*J P* lines are shown in Figures 4 and 5 (*solid lines*), respectively. In these figures, the individual lines that contribute to the average are shown as histograms. The points that are included in the average are indicated by asterisks. The distribution of the asterisks shows that many of the deviant points are excluded by the weighting scheme, as desired. For both the low-*J R* and high-*J P* lines, the average line profile indicates that the CO emission extends to approximately ± 90 km s^{-1}. The location of the "horns" of the profile (at approximately ± 30–45 km s^{-1}) further indicates that the CO emission arises from a limited range of disk radii ($R_{\rm out}/R_{\rm in} \sim 5$–9).

3.3. *Disk Emission Model*

To estimate the range of disk radii from which the emission originates and the excitation conditions therein, we modeled the residual (stellar photosphere-subtracted) CO emission using a simple model of emission from a gaseous disk under the assumption of Keplerian rotation and thermal level populations (e.g., Carr et al. 1993; Najita et al. 1996). Given the estimated extinction of $A_V = 1.1$ (Furlan et al. 2006), we assumed a negligible extinction at 4.7 μm. For simplicity, no underlying continuum was assumed in fitting the line emission. This is reasonable given our limited goal of estimating the radial extent of the emitting gas.

An important model parameter is the stellar mass. We can estimate the stellar mass of V836 Tau both from pre–main-sequence

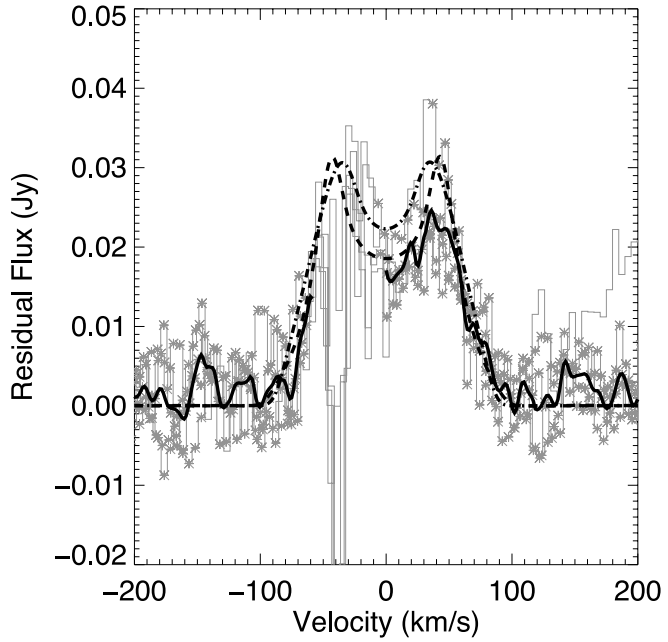

FIG. 5.—Average CO emission profile from V836 Tau in the 4.6 μm region (*heavy solid black line*) compared with a synthetic disk emission profile for the $v = 1-0$ *R*3 line in a model that has an outer radius to the emission (*dashed line*; see Fig. 6 and text for details). The synthetic *R*3 line profile for a model with a steep temperature gradient (*dash-dotted line*) is also shown (see text for details). The velocities shown are relative to the stellar velocity of V836 Tau. The individual lines that contribute to the average (1–0 *R*1–*R*4 and *R*6) are shown as gray histograms. Points included in the average are indicated by asterisks. Note that the region around the Pfβ line, located next to the 1–0 *R*1 line, was excluded from the average. Strong telluric CO absorption at -36 km s^{-1} is present in all of the profiles, so there is no average line profile in the surrounding velocity interval. [*See the electronic edition of the Journal for a color version of this figure*.]

evolutionary tracks and from available dynamical mass estimates of pre–main-sequence stars of the same spectral type and similar age. The K7 $\pm$ 1 spectral type (or $T_{\rm eff} = 4000 \pm 200$ K; White & Hillenbrand 2004) corresponds to a mass of $0.71^{+0.24}_{-0.18}\ M_\odot$ using the evolutionary tracks of Siess et al. (2000). Similarly, other T Tauri stars in Taurus with K7 spectral types have measured dynamical masses (Simon et al. 2000) of 0.72 $M_\odot$ (DL Tau) and 0.84 $M_\odot$ (GM Aur). Thus, the K7 dynamical masses and HR diagram position of V836 Tau are consistent with a stellar mass of 0.7–0.8 $M_\odot$. If the spectral type is larger or smaller by one subclass, a larger range in mass is allowed (0.5–1.0 $M_\odot$). Here, we assume a stellar mass of 0.75 $M_\odot$.

An additional model parameter is the system inclination, which we can obtain from the stellar rotation period $P_{\rm rot}$ of 6.76 days determined from long-term monitoring (Grankin et al. 2008), the projected stellar rotational velocity $v_* \sin i$ (12.1 km s^{-1}; White & Hillenbrand 2004), and the stellar radius R_*. These are related by

$$v_* \sin i = \frac{2\pi R_*}{P_{\rm rot}} \sin i.$$

The stellar radius can be estimated from the measured stellar luminosity and temperature. The stellar luminosity, obtained by integrating the stellar component in the SED fit (Fig. 3; see also Furlan et al. 2006), is 0.58 $L_\odot$ at the average Taurus distance of 140 pc, with a range of 0.46–0.87 $L_\odot$ if we account for the range in distances (126–173 pc) derived to individual Taurus objects (Bertout & Genova 2006). For $T_{\rm eff} = 4000 \pm 200$ K, $R_* = 1.6^{+0.40}_{-0.22}\ R_\odot$, where the uncertainty in the stellar temperature dominates the error on the low-luminosity end, and the uncertainty in the distance dominates the error on the high-luminosity end. An examination of all of the uncertainties in the above properties gives a possible inclination range of 55°–90°. Since V836 Tau does not have the extreme colors of an edge-on disk system (e.g., D'Alessio et al. 2006), we assume a more modest inclination of 65° for the modeling.

With these constraints on the stellar mass and system inclination, we can then infer the range of disk radii over which the emission arises assuming Keplerian rotation. The maximum velocity extent of the $v = 1-0$ CO emission lines ($v_{\rm max} \sim 90 \pm 10$ km s^{-1}; see § 3.2) and the inclination range of $i = 55° - 90°$ implies an inner radius of $R_{\rm in} = 0.05-0.09$ AU for the emitting gas. This range of $R_{\rm in}$ is consistent with the values of $R_{\rm in}$ measured for classical T Tauri stars using CO emission-line profiles (Najita et al. 2007a; Carr 2007). The overall shape of the emission-line profile further suggests that the emission extends out to a radius $\sim 6R_{\rm in}$, significantly less than the $>20R_{\rm in}$ that would be inferred from the centrally peaked CO fundamental emission profiles of most T Tauri stars (Najita et al. 2003). Thus, the outer radius of the V836 Tau CO emission is in the range 0.3–0.5 AU.

We can provide constraints on the mean conditions in the emitting gas by modeling the CO spectrum with a radially constant excitation temperature and column density. The similar shape and strength of the $v = 1-0$ emission lines over a wide range in J reveals that the emission lines are optically thick, i.e., that the gas column density is >0.001 g cm^{-2} if turbulent line broadening is negligible. In addition, the absence of detectable $v = 1-0$ ^{13}CO emission lines limits the column density to <0.03 g cm^{-2} for a CO abundance of 3×10^{-4} relative to hydrogen and an interstellar ^{13}CO/^{12}CO ratio of 90.

The weakness of the $v = 2-1$ and $v = 3-2$ lines in the spectrum requires either a low average excitation temperature or that the vibrational levels above $v = 1$ depart significantly from thermal equilibrium. For LTE level populations, the relative strengths of the $v = 1-0$ lines and the limit on the strength of the $v = 2-1$ transitions constrain the mean excitation temperature to the range 700–1100 K. Smaller excitation temperatures require larger emitting areas to produce the required line flux, as well as larger inclinations in order to produce the emission over the required range of velocities. As a result, at temperatures $\lesssim$700 K, the requirement on the line flux drives the emitting radii to values large enough that the required velocities cannot be obtained at any inclination. For a radially constant excitation temperature $\gtrsim$1200 K, the $v = 2-1$ lines are too strong relative to the $v = 1-0$ lines. In addition, given the constraints on the radial range (and therefore the emitting area) of the emission, the strength of the $v = 1-0$ lines are overpredicted at such high temperatures.

We can obtain a better fit to the average line profiles by allowing the temperature to vary as a function of radius. Consistent with the above considerations, a gas temperature that varies slowly with radius [$T = 1200\ {\rm K}(r/R_{\rm in})^{-0.30}$] and a line-of-sight disk column density of $\Sigma = 0.003$ g cm^{-2} that is radially constant between $R_{\rm in} = 13\ R_\odot$ and $R_{\rm out} = 5R_{\rm in}$, gives a reasonable fit to the spectra assuming LTE level populations (Fig. 6). In addition to providing a reasonable fit to the relative line strengths of the $v = 1-0$ lines, the model also reasonably fits the average line profiles of the $v = 1-0$ lines (Figs. 4 and 5, *heavy dashed lines*).

We can also fit the spectra with a model that uses a steep temperature gradient rather than a specified outer radius to limit the radial extent of the emission. With a temperature profile $T = 1400\ {\rm K}(r/R_{\rm in})^{-0.6}$ and a radially constant line-of-sight column density $\Sigma = 0.0037$ g cm^{-2} and $R_{\rm in} = 16.2\ R_\odot$, the 1–0 emission

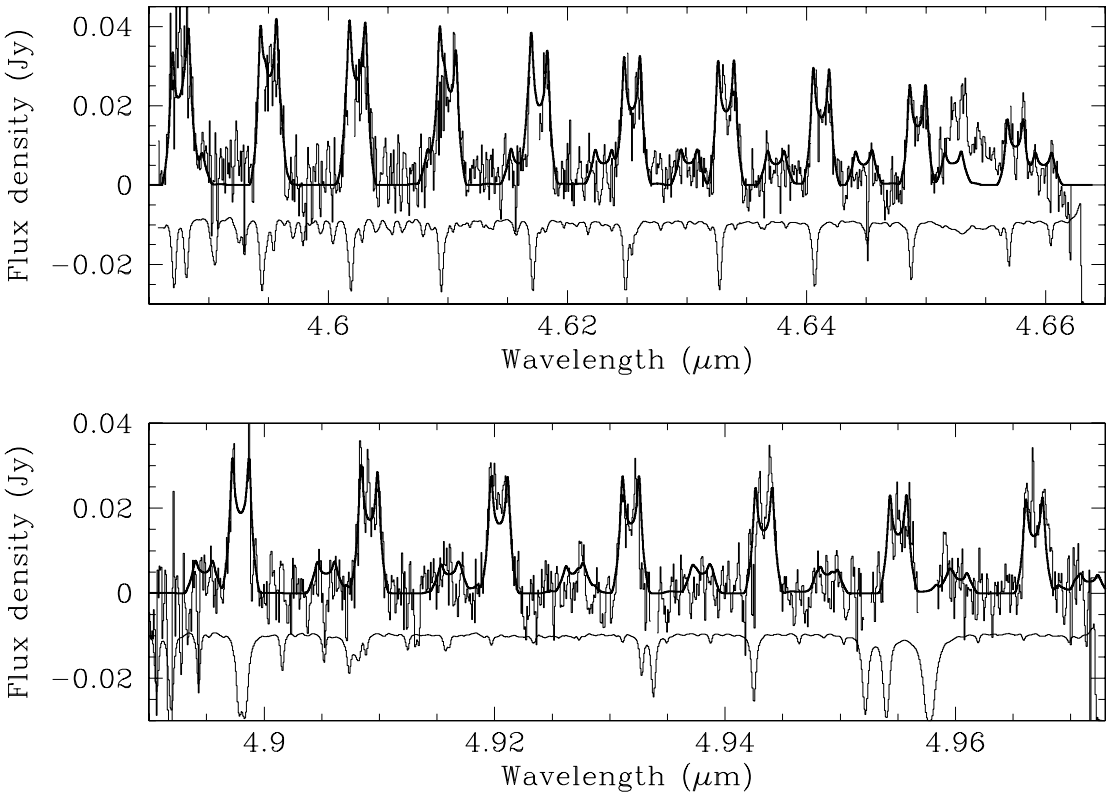

FIG. 6.—CO emission spectrum from V836 Tau (*black histogram*) in the 4.6 μm (*top*) and 4.9 μm (*bottom*) regions compared with a model disk emission spectrum (*red line*) in which the emission is truncated at $R_{out} = 5R_{in}$ (see text for details). Regions of poor telluric correction, as indicated by the telluric transmission spectrum (*lower blue line*), have been excised from the plotted observed spectrum. [*See the electronic edition of the Journal for a color version of this figure*.]

decreases sharply beyond $7R_{in}$–$8R_{in}$ because the Planck function contributes little at 4.7 μm at the low temperatures achieved at these radii ($\lesssim$400 K). The high-J P-branch lines are also optically thin at these radii. The model provides a reasonable fit to the relative strengths of the $v = 1$–0 lines. The average line profiles are reasonably well fit (Figs. 4 and 5, *heavy dash-dotted lines*), although the central dip in the $v = 1$–0 R lines is shallower than observed. This is because the low-J R lines remain optically thick (and continue to produce emission) to larger radii than the high-J P lines. In contrast, the outer radius to the emission used in the first model, produces similar line profiles for the low-J R and high-J P lines.

To summarize, the observed spectra can be explained with an abrupt truncation of the CO emission beyond an outer radius of $7R_{in}$–$8R_{in}$. A steep temperature gradient where the temperature drops to $\lesssim$400 K at $7R_{in}$–$8R_{in}$ is an alternative explanation. Note that there is a slight inconsistency in the model parameters used in the above fits. The adopted inclination formally implies a distance of 165 pc rather than the nominal Taurus distance of 140 pc that we have assumed in the fits. If V836 Tau is located at a larger distance than 140 pc, the CO emission can be fit with similar model parameters to those used above, with the modification that $M_* = 0.88\ M_\odot$ and the emission arises from radii 1.18 times larger than assumed above. The higher mass is within the mass range allowed by the uncertainty in the stellar spectral type.

4. DISCUSSION

4.1. *Truncated Excitation or Truncated Disk?*

The CO emission from V836 Tau shows similarly double-peaked line profiles for lines spanning a large range in excitation temperature. The line profile shapes indicate that the CO emission is truncated beyond $\sim$0.4 AU. The similarity in the relative strengths of the 1–0 transitions show that the 1–0 transitions are optically thick over the emitting region. As described in the previous section, these properties could be produced by a *physical* truncation of the gaseous disk beyond a radius of $\sim$0.4 AU or a truncation of the CO emission (but not the disk gas column density) at the same radius.

Although it is difficult to determine which of these interpretations is correct based on the available information, some possibilities can be ruled out. For example, the truncation of the CO emission is unlikely to result from the thermal dissociation of CO since the excitation temperature of the gas is much less than the thermal dissociation temperature of CO ($\sim$4000 K at the densities of inner disks).

We might also consider the possible explanations that have been put forward for the origin of the double-peaked line profiles observed in the $v = 2$–0 CO overtone band-head emission from T Tauri stars and Herbig Ae stars at 2.3 μm (e.g., Carr et al. 1993; Najita et al. 1996, 2000). Such emission is detected only from sources with high accretion rates, probably a consequence of the temperatures and high column densities that are needed to produce the overtone emission. Since these systems have disks that are believed to be radially continuous, the double-peaked lines are unlikely to arise from a radially truncated disk. We have previously described two possible explanations for the double-peaked lines that make up the CO $v = 2$–0 band head: (1) the outer radius is a dust sublimation front, or (2) the transition from atomic H to H_2 at decreasing temperature depopulates the higher CO vibrational levels.

In the first scenario, a dust sublimation front renders the line-emitting layer optically thick in the continuum at temperatures below $\sim$1500 K, eliminating the contrast of the CO $v = 2$–0

emission above the continuum at these radii (e.g., Carr 1989). This explanation is difficult to apply to the CO fundamental lines, because typical dust temperatures at the inferred outer radius of ∼0.4 AU for the CO fundamental emission are much below the dust sublimation temperature (e.g., D'Alessio et al. 1999) and measured dust sublimation radii are much smaller than the inferred outer radius of the CO fundamental emission (Eisner et al. 2005; Muzerolle et al. 2003). Therefore, the outer radius observed for the CO fundamental emission is unlikely to result from dust sublimation.

As an alternative scenario, we previously speculated that the transition from atomic to molecular hydrogen at decreasing disk temperature leads to the depopulation of the higher vibrational levels of CO due to the lower collisional cross-section of molecular hydrogen with CO compared to that of atomic hydrogen with CO (Najita et al. 1996). In chemical equilibrium, disks would transition from a mixture of CO and atomic hydrogen at small disk radii ($T > 2000$ K) to a mixture of CO and molecular hydrogen at large disk radii ($T < 2000$ K). In this situation, we estimated that radiative trapping would be able to maintain the $v \geq 2$ vibrational populations down to a temperature of ∼1500 K, below which significant depopulation would occur. Using a non-LTE model of this kind, we were able to reproduce the line intensities and shapes of CO overtone emission lines covering a wide range of excitation conditions ($v = 2$–0 to $v = 5$–3) in the spectra of two Herbig Ae stars.

The same effect is unlikely to apply in detail to the truncation of the CO fundamental emission seen in V836 Tau ($R_{\rm out} \sim 0.4$ AU). While chemical equilibrium may be relevant at the large column densities needed to produce the overtone emission, disks are expected to have significant vertical structure and to depart significantly from chemical equilibrium at the smaller column densities needed to produce the fundamental emission. Thermal-chemical models of T Tauri disks irradiated by stellar X-rays (Glassgold et al. 2004; Meijerink et al. 2008) indicate that overlying the large column densities where the overtone lines form is a warm surface layer that is expected to be conducive to the production of CO fundamental emission over a large range in radii (Glassgold et al. 2004).

The X-ray-irradiated disk models, which have currently studied the structure of disks over the region 0.25–2 AU, find that throughout this range of radii disks possess a warm (∼1000 K) surface layer ($\gtrsim 10^{21}$ cm^{-2}) of CO mixed with atomic hydrogen (Glassgold et al. 2004; Meijerink et al. 2008). Thus, the CO fundamental transitions could plausibly be excited over radii within and beyond 1 AU. This expectation is in agreement with observations of CO fundamental emission from T Tauri stars. Empirically, we find that almost all accreting T Tauri stars show CO fundamental emission and that the majority of CO fundamental emission profiles are centrally peaked. This indicates that the emission arises from a wide range of disk radii ($R_{\rm out}/R_{\rm in} > 20$, $R_{\rm out} \simeq 1$–2 AU), without a sharp truncation in excitation as a function of velocity (Najita et al. 2003).

However, it is possible that these general trends, obtained for typical T Tauri stars, do not apply to V836 Tau. Whereas typical T Tauri stars have strong near-infrared excesses and stellar accretion rates $\sim 10^{-8}\,M_\odot$ yr^{-1}, V836 Tau has a weak near-infrared excess and a low stellar accretion rate $\sim 10^{-9}\,M_\odot$ yr^{-1} (Hartigan et al. 1995 scaled to Gullbring et al. 1998; Herczeg et al. 2006). The weak near-infrared excess might indicate either a significant settling of grains out of the disk atmosphere or a lack of dust at small disk radii.

In this situation, one might imagine that a lack of small grains could reduce the heating of the gaseous atmosphere, if gas-grain collisions dominate the heating of the gaseous disk. In a cooler atmosphere, vibrational CO emission would be more difficult to produce, perhaps contributing, thereby, to the truncation of the CO emission. This does not seem likely in the context of recent X-ray-irradiated disk atmosphere models, in which the gas is heated directly by X-rays or accretion-related processes and the grains function primarily as a coolant for the gas through collisions. In such a model, we might expect grain growth and settling to produce warmer gaseous atmospheres, rather than a radial truncation of the CO emission.

Alternatively, one might imagine that CO might be less abundant in a grain-poor disk atmosphere if the CO is synthesized from H_2 that forms on grains. However, in the X-ray-irradiated disk atmosphere models, the grains are typically warmer than 100 K within 1 AU, and have therefore been assumed to play no significant role in the synthesis of CO and other molecules (Glassgold et al. 2004). As a result, grain growth and settling is not expected to significantly reduce the strength of the CO emission from the disk atmosphere.

Another possibility is that the low accretion rate of V836 Tau compared to the average T Tauri accretion rate ($\sim 10^{-8}\,M_\odot$ yr^{-1}; Hartmann et al. 1998) might play a role in truncating the CO emission. Since accretion-related processes may heat the gaseous atmosphere (Glassgold et al. 2004), the gaseous atmosphere may experience reduced heating at the lower accretion rate of V836 Tau. While the available heating is clearly able to produce detectable $v = 1$–0 CO fundamental emission from V836 Tau, could reduced heating radially truncate the emission, perhaps via a non-LTE effect?

A simple estimate indicates that the vibrational populations could be in non-LTE. The critical density $n_{\rm cr}$ for the $v = 1$ level of CO, obtained from the Einstein A-values for the $v = 1$–0 transitions (e.g., Goorvitch & Chackerian 1994) and the $v = 1$–0 collision rates for CO with atomic hydrogen (Glass & Kironde 1983), varies as $T^{-1/2}$ and equals $\sim 5 \times 10^{12}$ cm^{-3} at a temperature of 1000 K (see discussion in Najita et al. 1996). Our modeling of the CO emission from V836 Tau shows that the $v = 1$–0 CO emission arises from a gas column density ∼0.01 g cm^{-2} at disk radii $\lesssim 0.4$ AU. In the D'Alessio et al. (1999) disk model, the density in the disk atmosphere over this range of column density is $n_{\rm H} \sim 10^{11}$–10^{12} cm^{-3} at radii 0.1–0.4 AU. Therefore, a rough estimate is $n_{\rm H}/n_{\rm cr} \sim 0.1$ in the CO emitting region.

Our modeling of the CO emission further shows that the $v = 1$–0 CO lines are optically thick, with $\tau \sim 10$. Since the escape probability for Gaussian lines depends asymptotically on the line optical depth as $\sim \tau^{-1}$ (Mihalas 1978), the line optical depth approximately compensates for the low value of $n_{\rm H}/n_{\rm cr}$ so that the $v = 1$ level could be in LTE. The situation for the higher vibrational levels is possibly similar, with the critical densities for these levels being comparable to the critical density for $v = 1$. This because the A-values of the higher vibrational levels are larger (proportional to v), but the collision rates may also be larger because of the contribution from $\Delta v > 1$ collisions (A. Glassgold 2008, private communication). Thus, the CO vibrational level populations could plausibly be in LTE, consistent with the assumption made in § 3.3.

However, both lower temperatures and lower densities in the CO emitting region will tend to drive departures from LTE. Reduced accretion heating can produce both lower temperatures and lower densities. As the accretion heating is reduced, the vertical temperature inversion that puts the CO into emission will become increasing limited to the lower column density surface region that can be heated by external irradiation (e.g., by stellar X-rays). This surface region will be characterized by lower

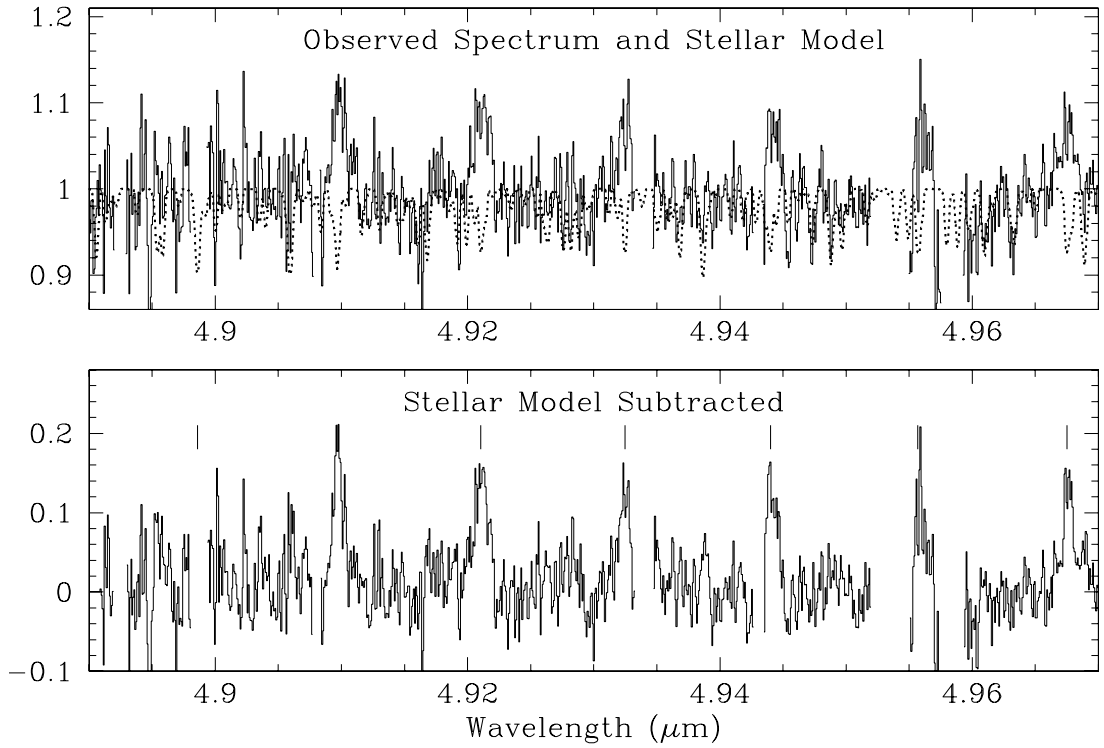

FIG. 7.—Same as in Fig. 2, but for LkCa 15. The wavelengths of CO $v = 1-0$ lines at the stellar velocity of LkCa 15 are indicated in the bottom panel (*short vertical lines*). While LkCa 15 is similar to V836 Tau in having a relatively low stellar accretion rate, its CO line profile is centrally peaked rather than double-peaked. [*See the electronic edition of the Journal for a color version of this figure.*]

densities. Detailed calculations of the thermal, chemical, and density structure of disk atmospheres are needed to address this issue quantitatively.

Because such calculations are currently lacking, we might take instead a more empirical approach and compare the CO fundamental line profiles of V836 Tau with those of other T Tauri stars with low stellar accretion rates and/or low near-infrared excesses. As an example of such a comparison, Figure 7 (*top*) shows the CO fundamental emission from LkCa 15, a T Tauri star with a stellar accretion rate similar to that of V836 Tau (Hartmann et al. 1998; see also Najita et al. 2007b). The spectrum shows the data reported in Najita et al. (2003), but rereduced using the approach described in § 2. The $v = 1-0$ CO emission from LkCa 15 is centered at the stellar velocity (*short vertical lines in bottom panel*), but compared to V836 Tau, it shows a centrally peaked profile.

Although the signal-to-noise ratio of the spectrum is limited, weak stellar photospheric features appear to be present. In the bottom panel of Figure 7, we show the CO emission from LkCa 15 after correction for a stellar photospheric contribution, following the approach described in § 3.1. The stellar photospheric model assumes an Allard stellar atmosphere model with a gravity of $\log g = 4.0$, an effective temperature of 4400 K to match the K5 spectral type of LkCa 15 (Herbig & Bell 1988), a stellar rotational velocity $v \sin i = 12.5$ km s^{-1} (Hartmann et al. 1987), and an observed (topocentric) radial velocity of -39.8 km s^{-1}, which is appropriate for the measured stellar radial velocity (Hartmann et al. 1987) and the observation date. A veiling of 2.5 times the stellar continuum roughly reproduces the strength of the stellar photospheric features near the 1–0 *P*30 line. This level of veiling is also consistent with the veiling at 5 μm implied by the SED (e.g., Furlan et al. 2006). Subtracting the veiled stellar photospheric component produces a disk CO emission profile that is even more centrally peaked (Fig. 7, *bottom*).

In addition to its low stellar accretion rate, LkCa 15 is also similar to V836 Tau in that it has the characteristics of a transition object with a weak near-infrared continuum and an optically thick outer disk (e.g., Bergin et al. 2004; Espaillat et al. 2007a). Its properties therefore probe empirically how both the reduction in small grains and reduced accretion-related heating might affect the CO fundamental emission from the disk. The LkCa 15 spectrum shows that in at least some cases, these effects do not radially truncate the CO fundamental emission within 1 AU.

To summarize, the double-peaked line profile of the CO fundamental emission from V836 Tau may indicate that the gaseous disk extends from close to the star ($\sim$0.05 AU) out to a physical truncation radius ($\sim$0.4 AU). If the gaseous disk in V836 Tau is instead continuous beyond this radius, the double-peaked CO profile would indicate a sudden truncation of the CO emission beyond a radius of 0.4 AU. As discussed in § 4.2, an abrupt decrement in excitation is not expected empirically, since the majority of CO emission profiles observed to date (both typical classical T Tauri stars and transition objects like LkCa 15) show centrally peaked CO profiles with no comparable decrement in excitation with radius.

However, a truncated emission profile may result from either an (anomalously) steep temperature gradient or departures from LTE that become important in low accretion rate systems. These two possible explanations can be explored and potentially distinguished with a higher signal-to-noise spectrum that measures the strengths of the $v = 2-1$ lines. A theoretical study of the possibility of non-LTE CO level populations would also be welcome in sorting out whether an excitation effect is a possible explanation for the outer radius of the emission. Additional observations of low accretion rate sources would be useful in exploring this issue empirically.

Most definitive of all would be observations of spectral line transitions that robustly probe the disk atmosphere of V836 Tau

at excitation temperatures <400 K. These observations would complement the insensitivity of the CO fundamental transitions to low-temperature gas. If little emission is detected with these diagnostics at disk radii >0.4 AU, that would strongly suggest that the gaseous inner disk in V836 Tau is physically truncated at ∼0.4 AU. Some of the mid-infrared molecular emission diagnostics recently reported in the spectrum of AA Tau (C_2H_2, HCN, H_2O, OH; Carr & Najita 2008) may prove useful in this regard.

4.2. *Nature of V836 Tau*

The possibility that the disk of V836 Tau is physically truncated beyond 0.4 AU may bear on our understanding of the nature of the system. As noted in § 1, V836 Tau has been previously classified as a transition object (Strom et al. 1989), a system with an optically thin inner disk (within $R_{\rm hole}$) and an optically thick outer disk (beyond $R_{\rm hole}$). The SEDs of these systems have been variously explained as a consequence of grain growth and planetesimal formation (e.g., Strom et al. 1989; Dullemond & Dominik 2005), giant planet formation (e.g., Skrutskie et al. 1990; Marsh & Mahoney 1992), or photoevaporation (e.g., Clarke et al. 2001; Alexander et al. 2006).

While all of these processes can produce optically thin regions in the disk (inner holes or gaps), they make different predictions for stellar accretion rates and disk masses, as well as the radial distribution of the gaseous disk. As a result, measuring the radial distribution of disk gas and comparing the stellar accretion rates and disk masses of transition objects with those of accreting T Tauri stars of comparable age can potentially sort among the possible explanations for a transitional SED. For example, a recent study using the latter approach showed that transition objects in Taurus (including V836 Tau) have stellar accretion rates that are on average ∼10 times lower than those of nontransitional T Tauri stars with comparable disk masses (Najita et al. 2007b). Such a reduced stellar accretion rate is predicted for disks that have formed Jovian mass planets (e.g., Lubow & D'Angelo 2006), suggesting that giant planet formation may play a role in explaining the origin of at least some transition objects.

Studies of the radial distribution of the gaseous disk in the system provide an additional way to distinguish the nature of individual transition objects. For example, although grain growth can render the inner disk optically thin (within $R_{\rm hole}$), the gas in the same region of the disk is not expected to be altered significantly; gas would therefore fill the region within $R_{\rm hole}$. If a giant planet has formed with a mass sufficient to open a gap, both the gas and dust would be expected to be cleared dynamically from the vicinity of the orbit of the planet, creating an inner disk (within $R_{\rm inner} < R_{\rm hole}$) that is fed by accretion streams from an outer disk (beyond $R_{\rm hole}$; Lubow et al.1999; Bryden et al. 1999; Kley 1999; D'Angelo et al. 2003; Lubow & D'Angelo 2006). Accretion streams are not expected in the case of a massive giant planet (∼10 $M_{\rm J}$; e.g., Lubow et al. 1999), and no significant gas or dust is expected anywhere within $R_{\rm hole}$ in this case. A lack of gas or dust within $R_{\rm hole}$ is also expected in the photoevaporation case; such systems are further expected to have a very low disk mass (∼0.001 $M_\odot$; e.g., Alexander & Armitage 2007).

Our results for V836 Tau are intriguing in this context. Compared to the SEDs of well-studied transition objects such as GM Aur and DM Tau, where a strong infrared excess appears only beyond ∼10 μm indicating an optically thin region 3–20 AU in size (Calvet et al. 2005), the SED of V836 Tau shows a significant infrared excess at a shorter wavelength ∼5–10 μm. Therefore, if the V836 Tau system has an optically thin inner region, it is comparatively small and plausibly within the range of disk radii probed by CO fundamental emission (within ≲2 AU; Najita et al. 2003). The SED of V836 Tau can be fit with a simple model of a flared optically thick disk with an inner hole ∼1 AU in radius (see Appendix). In comparison, the SED of the transition object LkCa 15 can be interpreted as indicating an optically thin region within ∼3 AU (Bergin et al. 2004), or a radial gap extending from 5–46 AU (Espaillat et al. 2007a). A planet orbiting at such large distances (∼3 AU or ∼40 AU) may create a gap in the disk, but not radially truncate the gaseous disk significantly within 1 AU. In contrast, systems like V836 Tau, in which the SED may indicate an optically thin region at much smaller radii (<1 AU), are the ones for which the CO fundamental emission would in principle be capable of diagnosing a physically truncated inner disk if an orbiting companion is present. The radially truncated CO emission that we observe may support this picture.

As an alternative interpretation of the available data, the short wavelength SED of V836 Tau ($\lambda < 10$ μm) can also be fit with a simple model of an inclined ($i = 60$), geometrically flat disk (see Appendix) that possibly results from significant grain growth and settling. In such a situation, the gaseous disk would be radially continuous and we might expect to observe a CO profile like those of other nontransition T Tauri stars. Such a profile, typically centrally peaked, is not observed.

In the photoevaporation and massive giant planet scenarios for the origin of a transitional SED, little gas is expected to be present within $R_{\rm hole}$, in contrast to the observed situation where a gaseous disk is present at 0.05–0.4 AU and ongoing (possibly intermittent) stellar accretion is observed. The relatively high disk mass of V836 Tau (∼0.01 $M_\odot$; Andrews & Williams 2005), compared to the much smaller masses at which photoevaporation is expected to be able to create an inner hole (∼0.001 $M_\odot$), further argues against the photoevaporation scenario. The possibility of a massive planet is also restricted by current limits on the stellar radial velocity of V836 Tau, which constrain the mass of a companion within 0.4–1 AU to <5−10 $M_{\rm J}$ (L. Prato 2008, private communication).

These arguments are schematic in that they rely on theoretical predictions that have not been verified observationally. For example, the sizes of gaps that will be induced by an orbiting companion of a given mass, and the extent to which stellar accretion will be reduced, are poorly known from an observational point of view. Stellar companions have been found to establish large inner holes and to terminate stellar accretion in some transition objects (CoKu Tau/4; Ireland & Kraus 2008; D'Alessio et al. 2005) and not in others (CS Cha; Guenther et al. 2007; Espaillat et al. 2007b). The situation for lower mass companions is essentially unexplored. As theoretical predictions are tested, it will be useful to examine in detail the range of companion masses that are consistent with the properties of V836 Tau.

5. SUMMARY AND FUTURE DIRECTIONS

V836 Tau has been classified as a transition object (Strom et al. 1989), a system that may be on the verge of dissipating its disk, possibly as a consequence of planetesimal formation or giant planet formation. These processes can reduce the continuum opacity in certain regions of the disk, producing an optically thin inner hole or a low column density gap. If V836 Tau has such an optically thin region, the weak near-infrared excess and the stronger 10 μm excess in the system indicates that the optically thin region is much smaller (<1 AU) than the optically thin region in well-studied transition objects such as GM Aur and DM Tau (Calvet et al. 2005), where the optically thin region is 3–20 AU in radius. Thus CO fundamental emission, which probes the region ≲2 AU (Najita et al. 2003), can potentially map out the radial structure of the inner gaseous disk in V836 Tau to determine,

for example, if the inner disk has been truncated by a companion orbiting within 1 AU.

Along these lines, we find that the $v = 1–0$ CO fundamental line profiles of V836 Tau are unusual compared to those of other T Tauri stars in being markedly double-peaked. The strength and shape of the line emission is consistent with emission from a Keplerian disk over a limited range of radii ($\sim$0.05–0.4 AU). Further work is needed to determine whether the outer radius of the emission results from the physical truncation of the disk beyond $\sim$0.4 AU or the truncated excitation of the $v = 1–0$ CO fundamental transitions beyond this radius.

A theoretical approach to this problem requires studies of the thermal, chemical, and excitation structure of disks at a level of detail that is appropriate for comparison with observations. Studies of the possibility of non-LTE CO level populations in low accretion rate systems would be particularly welcome. For a more empirical approach to the problem, we might compare the observed line profiles of V836 Tau with other low accretion rate systems in which the disk is expected to be radially continuous within a few AU. As an example of the latter approach, we discussed the CO fundamental line profiles of LkCa 15, a T Tauri star with a low accretion rate similar to that of V836 Tau. The more centrally peaked line profiles of LkCa15, if representative of other low accretion rate systems, would suggest that the double-peaked emission profiles of V836 Tau arise from a physically truncated inner disk.

Such a physically truncated inner disk might arise if the system has formed a Jovian mass planet that has cleared a gap in the disk. A simple fit to the SED of V836 Tau is consistent with a flared disk that has an optically thin region within $\sim$1 AU. Thus, a possible interpretation of the data is that an orbiting companion has created a gap between a gaseous inner disk within 0.4 AU and an optically thick outer disk beyond 1 AU. Since the above fit to the SED is nonunique, it would be useful to use both improved SED modeling techniques (e.g., Calvet et al. 2005) and infrared interferometry (e.g., Ratzka et al. 2007) to test the hypothesis that the dust disk has an optically thin gap or inner hole.

In systems that have formed a Jovian mass planet, small grains may be filtered out of the inward accretion flow at the outer edge of the gap (Rice et al. 2006), rendering the dust distribution a poor tracer of the physical structure of the disk at smaller radii. Gaseous disk tracers, like the CO fundamental emission discussed here, may then be *needed* to probe disk structure at these smaller radii. Thus, there is considerable motivation to expand the study of gaseous disk diagnostics beyond the present case, to understand more generally whether and how well diagnostics such as CO fundamental emission can probe the radial structure of gaseous disks.

We are grateful to Steve Strom for stimulating and insightful discussions on this topic. We also thank Lisa Prato for communicating her radial velocity results in advance of publication. Financial support for this work was provided by the NASA Origins of Solar Systems program (NNH07AG51I) and the NASA Astrobiology Institute under Cooperative Agreement No. CAN-02-OSS-02 issued through the Office of Space Science. This work was also supported by the Life and Planets Astrobiology Center (LAPLACE). Basic research in infrared astronomy at the Naval Research Laboratory is supported by 6.1 base funding. The authors wish to recognize and acknowledge the very significant cultural role and reverence that the summit of Mauna Kea has always had within the indigenous Hawaiian community. We are most fortunate to have the opportunity to conduct observations from this mountain.

APPENDIX

RADIAL DUST DISTRIBUTION

The low stellar accretion rate of V836 Tau ($\sim 10^{-9}\ M_\odot\ \mathrm{yr}^{-1}$; from Hartigan et al. [1995], scaled downward by a factor of $\sim$10 as in Najita et al. [2007b] or Gullbring et al. [1998]) suggests that the disk temperature distribution will be dominated by the passive reprocessing of stellar radiation. Accordingly, simple SEDs fits suggest that the short wavelength SED can be fit either as a passive optically thick disk that is flat at small radii and radially continuous (Fig. 8) or as a passive, flared optically thick disk with an inner hole (Fig. 9).

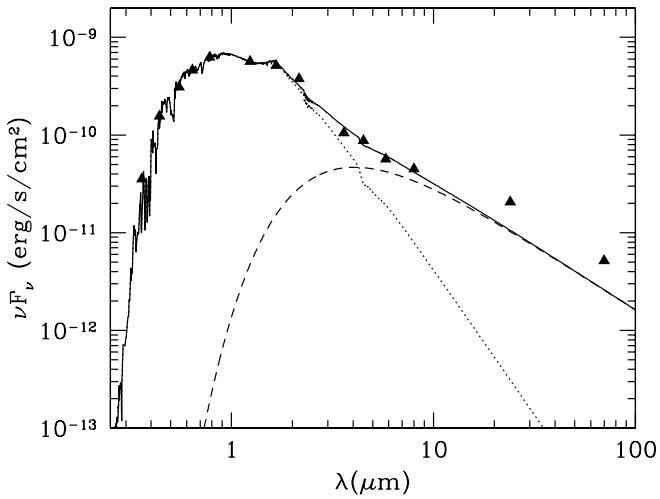

FIG. 8.—Dereddened SED of V836 Tau (*triangles*) compared with the SED produced by a flat reprocessing disk (*dashed line*) and a model photosphere (see Fig. 3; *dotted line*) observed at $i = 60$.

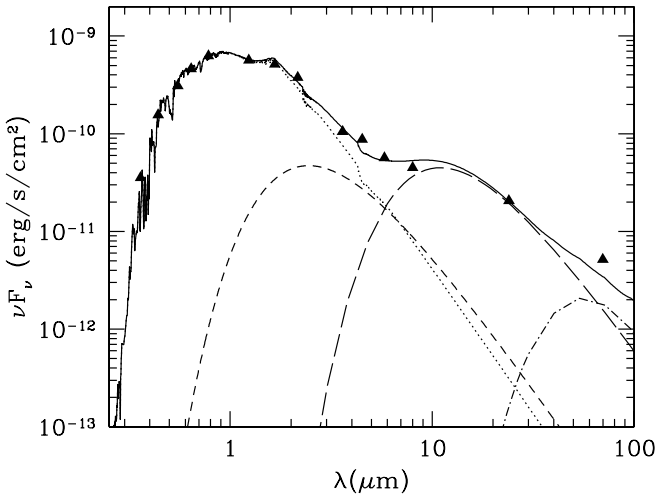

FIG. 9.—Fit to the dereddened SED of V836 Tau (*triangles*) obtained by combining a model stellar photosphere (see Fig. 3, *dotted line*), with the SED of a flared reprocessing CGPLUS disk that is truncated at 1.1 AU, and a 1500 K blackbody that represents residual dust within 1 AU (*short-dashed line*). An inclination of $i = 60$ is assumed. The CGPLUS model includes contributions from the disk wall (*long-dashed line*), the disk surface (*dash-dotted line*), and the disk midplane (not shown). The model assumes that the scale height of the disk is χ times the pressure scale height where $\chi = 1.25$ at the wall and $\chi = 0.6$ at larger disk radii.

In the former case, the 3–8 μm IRAC excesses are well fit with a continuous flat disk, observed at an inclination $i = 60$, that has a temperature distribution $T_D \propto r^{-3/4}$ with a normalization appropriate to a passive reprocessing disk (e.g., Adams et al. 1988). The disk is assumed to be optically thick beyond the dust sublimation radius (where $T_D = 1500$ K) and to have negligible optical depth within that radius (<0.017 AU). While the 3–9 μm excess is well fit and arises from disk radii within 0.5 AU, the excesses at 24 and 70 μm are underpredicted. A disk that is more strongly flared beyond $\sim$0.5 AU would likely produce a better fit. While such a simple model does a reasonable job fitting the short wavelength SED, it implies that the inner radius of the dust disk (at 0.017 AU) is within the inner radius of the CO emission (at $\sim$0.05 AU; § 3.3). This is in contrast to the situation found for more active T Tauri stars, where the SED is better fit with a frontally illuminated hot inner dust rim located further from the star (at $\gtrsim$0.1 AU). Such structures can account for the magnitude of the near-infrared excesses of T Tauri stars (Muzerolle et al. 2003). They also agree with the dust inner radii measured using infrared interferometry (e.g., Eisner et al. 2005).

To illustrate the latter case, we fit the SED using the public domain version of the CGPLUS modeling program written by C. P. Dullemond, C. Dominik, and A. Natta to calculate the disk contribution.[2] The CGPLUS model is based on the models of Chiang & Goldreich (1997) and Dullemond et al. (2001). The model includes four physical components: a stellar blackbody, a puffed-up inner rim, the disk surface, and the disk interior. Figure 9 shows the contribution to the SED of a disk truncated at an inner rim temperature of 330 K, corresponding to a disk radius of 1.1 AU. The inner rim (*long-dashed line*) is modestly flared ($\chi_{\rm rim} = 1.25$), and the rest of the disk is less strongly flared ($\chi_{\rm disk} = 0.6$). While the stellar blackbody was used in calculating the temperature of the other components, in constructing the composite SED we used a Basel stellar atmosphere (ver. 2.2, corrected; Lejeune 2002) of the same effective temperature. Adding a hot blackbody component $T = 1500$ K (*short-dashed line*), representing hot dust located close to the star, produces a reasonable fit to the SED. There is significant degeneracy in the model parameters, as might be expected given the number of parameters in the CGPLUS model and the limited number of data points used in the fit. More restrictive fits could be obtained with a more sophisticated disk atmosphere model (e.g., D'Alessio et al. 2005), a self-consistent treatment of the inner and outer disk components, and constraints from interferometry (e.g., Ratzka et al. 2007).

[2] See http://www.mpia-hd.mpg.de/homes/dullemon/radtrans.

REFERENCES

Adams, F., Lada, C. J., & Shu, F. H. 1988, ApJ, 326, 865
Alexander, R. D., & Armitage, P. J. 2007, MNRAS, 375, 500
Alexander, R. D., Clarke, C. J., & Pringle, J. E. 2006, MNRAS, 369, 229
Andrews, S. M., & Williams, J. P. 2005, ApJ, 631, 1134
Bergin, E., et al. 2004, ApJ, 614, L133
Beristain, G., Edwards, S., & Kwan, J. 2001, ApJ, 551, 1037
Bertout, C., & Genova, F. 2006, A&A, 460, 499
Blake, G. A., & Boogert, A. C. A. 2004, ApJ, 606, L73
Brittain, S. D., Simon, T., Najita, J. R., & Rettig, T. W. 2007, ApJ, 659, 685
Bryden, G., Chen, X., Lin, D. N. C., Nelson, R. P., & Papaloizou, J. C. B. 1999, ApJ, 514, 344
Calvet, N., et al. 2005, ApJ, 630, L185
Carr, J. S. 1989, ApJ, 345, 522
———. 2007, in IAU Symp. 243, Star-Disk Interaction in Young Stars, ed. J. Bouvier (Cambridge: Cambridge Univ. Press), 135
Carr, J. S., & Najita, J. R. 2008, Science, 319, 1504
Carr, J. S., Tokunaga, A. T., Najita, J., Shu, F. H., & Glassgold, A. E. 1993, ApJ, 411, L37
Chiang, E. I., & Goldreich, P. 1997, ApJ, 490, 368
Clarke, C. J., Gendrin, A., & Sotomayor, M. 2001, MNRAS, 328, 485
D'Alessio, P., Calvet, N., Hartmann, L., Franco-Hernández, R., & Servín, H. 2006, ApJ, 638, 314
D'Alessio, P., Calvet, N., Hartmann, L., Lizano, S., & Cantó, J. 1999, ApJ, 527, 893
D'Alessio, P., et al. 2005, ApJ, 621, 461
D'Angelo, G., Henning, T., & Kley, W. 2003, ApJ, 599, 548
Dullemond, C. P., Dominik, C., & Natta, A. 2001, ApJ, 560, 957
———. 2005, A&A, 434, 971
Duvert, G., Guilloteau, S., Ménard, F., Simon, M., & Dutrey, A. 2000, A&A, 355, 165
Eisner, J. A., Hillenbrand, L. A., White, R. J., Akeson, R. L., & Sargent, A. I. 2005, ApJ, 623, 952
Espaillat, C., Calvet, N., D'Alessio, P., Hernandez, J., Qi, C., Hartmann, L., Furlan, E., & Watson, D. M. 2007a, ApJ, 670, L135
Espaillat, C., et al. 2007b, ApJ, 664, L111
Furlan, E., et al. 2006, ApJS, 165, 568

Glass, G. K., & Kironde, S. 1983, J. Chem. Phys., 86, 908
Glassgold, A. E., Najita, J. R., & Igea, J. 2004, ApJ, 615, 972
Goorvitch, D. 1994, ApJS, 95, 535
Goorvitch, D., & Chackerian, C. 1994, ApJS, 91, 483
Grankin, K. N., Bouvier, J., Herbst, W., & Melnikov, S. Yu. 2008, A&A, 479, 827
Guenther, E. W., Esposito, M., Mundt, R., Covino, E., Alcalá, J. M., Cusano, F., & Stecklum, B. 2007, A&A, 467, 1147
Gullbring, E., Hartmann, L., Briceño, C., & Calvet, N. 1998, ApJ, 492, 323
Hartigan, P., Edwards, S., & Ghandour, L. 1995, ApJ, 452, 736
Hauschildt, P. H., Allard, F., & Baron, E. 1999, ApJ, 512, 377
Hartmann, L., Calvet, N., Gullbring, E., & D'Alessio, P. 1998, ApJ, 495, 385
Hartmann, L., Soderblom, D. R., & Stauffer, J. R. 1987, AJ, 93, 907
Herbig, G. H., & Bell, K. R. 1988, Lick Obs. Bull., 1111, 1
Herczeg, G. J., Linsky, J. L., Walter, F. M, Gahm, G. F., & Johns-Krull, C. M. 2006, ApJS, 165, 256
Ireland, M. J., & Kraus, A. L. 2008, ApJ, 678, L59
Kenyon, S. J., Brown, D. I., Tout, C. A., & Berlind, P. 1998, AJ, 115, 2491
Kenyon, S. J., & Hartmann, L. 1995, ApJS, 101, 117
Kley, W. 1999, MNRAS, 303, 696
Kurucz, R. L. 1993, Kurucz CD-ROM 13, ATLAS9 Stellar Atmosphere Programs and the 2 km/s Grid (Cambridge: SAO)
Lejeune, T. 2002, in ASP Conf. Proc. 274, Observed HR Diagrams and Stellar Evolution, ed. Lejeune, T., & Fernandes, J. (San Francisco: ASP), 159
Lubow, S. H., & D'Angelo, G. 2006, ApJ, 641, 526
Lubow, S. H., Seibert, M., & Artymowicz, P. 1999, ApJ, 526, 1001
Marsh, K. M., & Mahoney, M. J. 1992, ApJ, 395, L115
Mathis, J. S. 1990, ARA&A, 28, 37
McLean, I. S., et al. 1998, Proc. SPIE, 3354, 566
Meijerink, R., Glassgold, A. E., & Najita, J. 2008, ApJ, 676, 518
Mihalas, D. 1978, Stellar Atmospheres (San Francisco: Freeman)
Mundt, R., Walter, F. M., Feigelson, E. D., Finkenzeller, U., Herbig, G. H., & Odell, A. P. 1983, ApJ, 269, 229
Muzerolle, J., Calvet, N., Hartmann, L., & D'Alessio, P. 2003, ApJ, 597, L149
Najita, J., Carr, J. S., Glassgold, A. E., Shu, F. H., & Tokunaga, A. T. 1996, ApJ, 462, 919
Najita, J. R., Carr, J. S., Glassgold, A. E., & Valenti, J. 2007a, in Protostars and Planets V, ed. B. Reipurth (Tucson: Univ. Arizona Press), 507
Najita, J., Carr, J. S., & Mathieu, R. D. 2003, ApJ, 589, 931
Najita, J. R., Edwards, S., Basri, G., & Carr, J. 2000, in Protostars and Planets IV, ed. V. Mannings, A. P. Boss, & S. S. Russell (Tucson: Univ. Arizona Press), 457
Najita, J. R., Strom, S. E., & Muzerolle, J. 2007b, MNRAS, 378, 369
Padgett, D. L. 1996, ApJ, 471, 847
Padgett, D. L., et al. 2006, ApJ, 645, 1283
Ratzka, Th., Leinert, Ch., Henning, Th., Bouwman, J., Dullemond, C. P., & Jaffe, W. 2007, A&A, 471, 173
Rice, W. K. M., Armitage, P. J., Wood, K., & Lodato, G. 2006, MNRAS, 373, 1619
Santos, N. C., et al. 2008, A&A, 480, 889
Siess, L., Dufour, E., & Forestini, M. 2000, A&A, 358, 593
Simon, M., Dutrey, A., & Guilloteau, S. 2000, ApJ, 545, 1034
Skrutskie, M. F., Dutkevitch, D., Strom, S. E., Edwards, S., Strom, K. M., & Shure, M. A. 1990, AJ, 99, 1187
Sneden, C. 1973, Ph.D. thesis, Univ. Texas (Austin)
Strom, K. M., Strom, S. E., Edwards, S., Cabrit, S., & Skrutskie, M. F. 1989, AJ, 97, 1451
White, R. J., & Hillenbrand, L. A. 2004, ApJ, 616, 998
Wolk, S. J., & Walter, F. M. 1996, AJ, 111, 2066